Static and Dynamic Wetting Measurements of Single Carbon Nanotubes

Asa H. Barber
Department of Materials and Interfaces, Weizmann Institute of Science, Rehovot 76100, Israel

Sidney R. Cohen
Chemical Research Support, Weizmann Institute of Science, Rehovot 76100, Israel

H. Daniel Wagner
Department of Materials and Interfaces, Weizmann Institute of Science, Rehovot 76100, Israel
(Received 29 December 2003; published 7 May 2004)

Individual carbon nanotubes were immersed and removed from various organic liquids using atomic force microscopy. The carbon nanotube–liquid interactions could be monitored *in situ,* and accurate measurements of the contact angle between liquids and the nanotube surface were made. These wetting data were used to produce Owens and Wendt plots giving the dispersive and polar components of the nanotube surface.

DOI: 10.1103/PhysRevLett.92.186103 PACS numbers: 68.08.Bc, 81.05.Tp, 81.07.De

The surface properties of fibrous materials and their interactions with liquids have been the subject of numerous studies for decades. In particular, wetting of fibers has resulted in increased understanding of the behavior of curved surfaces with liquids [1]. Carbon nanotubes represent a new class of nanofibers with potential applications, such as structural reinforcement in polymer composites [2] or as conduits in nanofluidic systems [3]. For these types of applications it is imperative to understand the interactions between the nanotube and the liquid phase. This is generally difficult to assess experimentally due to the nanometer size of the tubes. Only a few studies have addressed this problem, on either a theoretical [4,5] or an experimental basis [3,6]. Such measurements either were qualitative [3] or, based on transmission electron microscopy (TEM) observations, which provides no real-time information, are technically incompatible with high vapor pressure liquids and have large uncertainties in assigned contact angle values [6]. Indeed, the measurement of liquid contact angles on microscopic fibers has been widely documented to contain significant errors [7], leading to numerous studies that address this issue (see [8]). A resulting experimental technique, involving immersing and removing a single fiber from a probe liquid, has been used previously to assess the liquid-fiber contact angle. This technique, an adaptation of the Wilhelmy balance method, has been shown to be effective in characterizing a range of fibers and is highly sensitive to different chemical treatments [9] of the fiber surface. We show here that it is possible to adapt this method to perform so-far unavailable measurements of the static and dynamic wetting characteristics of individual carbon nanotubes using a range of simple liquids in air.

Individual multiwalled carbon nanotubes (MWCNTs) grown by an arc-discharge method (Dynamic Enterprises, U.K.) were attached to calibrated [10] atomic force microscope (AFM) tips using previously described methods [11]. Each such nanotube had a diameter of approximately 20 nm. The nanotubes were selected in a high-resolution scanning electron microscope (SEM) prior to attaching to the AFM tip. The diameter of the nanotubes was thus accurately determined, to within 1 or 2 nm. A typical nanotube-AFM probe is shown in Fig. 1. Liquids of polydimethyl siloxane (PDMS), polyethylene glycol

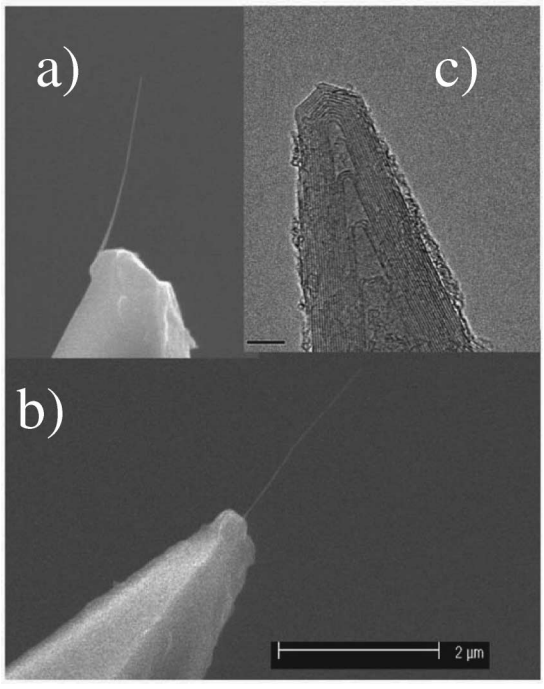

FIG. 1. High resolution scanning electron microscopy (SEM) pictures of a MWCNT-AFM tip from (a) the side, (b) 90° to the side, and (c) transmission electron microscopy (TEM) picture of a nanotube showing the closed end. Note that for successful wetting the nanotube attached to the AFM tip is relatively long and well aligned. Scale bar is 2 μm for the SEM pictures and 5 nm for the TEM pictures.

(PEG, $M_w = 400$), glycerol, and water were used as probe liquids in this study, with the liquid properties listed in Table I. The nanotube-AFM probes were carefully lowered into the various liquids in the AFM (NT-MDT, Russia) while monitoring the cantilever deflection signal. The nanotube was held in each liquid for approximately 10 s and then fully removed by retracting the sample surface with the z-piezo under AFM control. The force acting on the nanotube during immersion and retraction, monitored as the cantilever deflection signal, was recorded using a digital scope.

For PDMS the "jump-in" of the nanotube-AFM probe is observed to be large due to a complete and spontaneous wetting of the nanotube, up to and including the silicon AFM tip itself. This behavior (with PDMS) occurred regardless of the nanotube length. Similar behavior (spontaneous wetting) occurred with all the liquids when using bare silicon tips as a control, or tips where the attached nanotube was of length 0.5 μm or less. This resulted in the liquid engulfing the entire cantilever leading to the loss of the optical reflection signal at the measuring photodiode of the AFM. However, when the free nanotube length was significantly larger (exceeding 1 μm), only a portion of this length was wet by PEG, glycerol and water, allowing measurement of the wetting force.

Figure 2 shows the force profiles for individual nanotubes in the liquids. The left side of the profile corresponds to the nanotube being partially immersed in the liquid, with a constant and attractive wetting force acting on the nanotube. Retraction of the nanotube results in an increase of the attractive force, reflecting the increased bending of the cantilever toward the receding liquid surface, until the nanotube completely separates from the liquid and the force falls to zero. The portion of the curve over which the attractive force increases represents both removal of the submerged nanotube length from the liquid, and distortion of the liquid meniscus. This region, in the different liquids, corresponds to retraction distances ranging from 100 nm (PEG) to 500 nm (water). Initially, when the nanotube is partially immersed in the probe liquid, a finite equilibrium contact angle is established at the interface. The nanotube is restricted from becoming fully immersed in the liquid due to the restoring force of the AFM cantilever. We have assumed in this study that all liquids interact with the outer surface of the nanotube only, as supported by the TEM picture in Fig. 1(c), which shows that the nanotube structure is closed at the ends.

Any significant bending of the nanotube at the liquid surface would contribute to the measured cantilever deflection and must be considered together with the wetting force to properly interpret the force data. Qualitative observations of the wetting in an environmental SEM (not shown) corroborate the model presumed here of a straight nanotube, wet by a liquid meniscus. Furthermore, simple calculations show that Euler buckling for a case where the nanotube principle length axis is oriented perpendicular to the liquid surface or lateral bending due to a slight off-axis orientation of the nanotube requires a force which is at least 1 order of magnitude higher than the forces measured here, indicating that bending does not occur. Finally, unbending of the nanotube as the bent tube peels away from the liquid surface should result in a continuously decreasing tube-liquid interaction, leading to a monotonic drop in force, rather than the initial rise observed in Fig. 2.

A force balance can be used to calculate the equilibrium contact angle for each probe liquid:

$$F_r = \pi d \gamma_\ell \cos\theta, \tag{1}$$

where F_r represents the cantilever restoring force, d is the nanotube diameter, γ_ℓ is the surface tension of the probe liquid, and θ is the liquid-nanotube wetting angle. The results are shown in Table I. Note that PDMS has been assigned a zero contact angle due to complete and spontaneous wetting of the nanotube. The wetting angle becomes larger as the probe liquid becomes increasingly polar, with water exhibiting the largest contact angle (80°). This value is in excellent agreement with the value of 82° calculated for a nanotube of diameter 20 nm, using general solutions developed for contact angles on fibers down to the nanoscale [4]. This result confirms the effect of the curvature on the wetting behavior.

Further insights into the interactions between liquid and curved solid surfaces are demonstrated in terms of the dispersive and polar energy contributions in the equations of Owens and Wendt [12]. According to those equations, the polar and dispersive components of a surface can be calculated from liquid contact angles with the nanotube surface and the physical properties of each

TABLE I. Physical parameters for various probe liquids wetting individual carbon nanotubes. The contact angles are calculated from Eq. (1).

Probe liquid	γ_ℓ (mJ m^{-2})	γ_ℓ^d (mJ m^{-2})	γ_ℓ^p (mJ m^{-2})	Contact angle (°)	Work of deformation, W ($\times 10^{-15}$ mJ)
Polydimethyl-siloxane (PDMS)	25.1	22.7	2.4	0	N/A
Polyethylene-glycol (PEG)	48.3	29.3	19.0	57.4 ± 5.9	8.4
Glycerol	64.0	34.0	30.0	74.2 ± 3.6	40.6
Water	72.8	21.8	51.0	80.1 ± 3.6	137.0

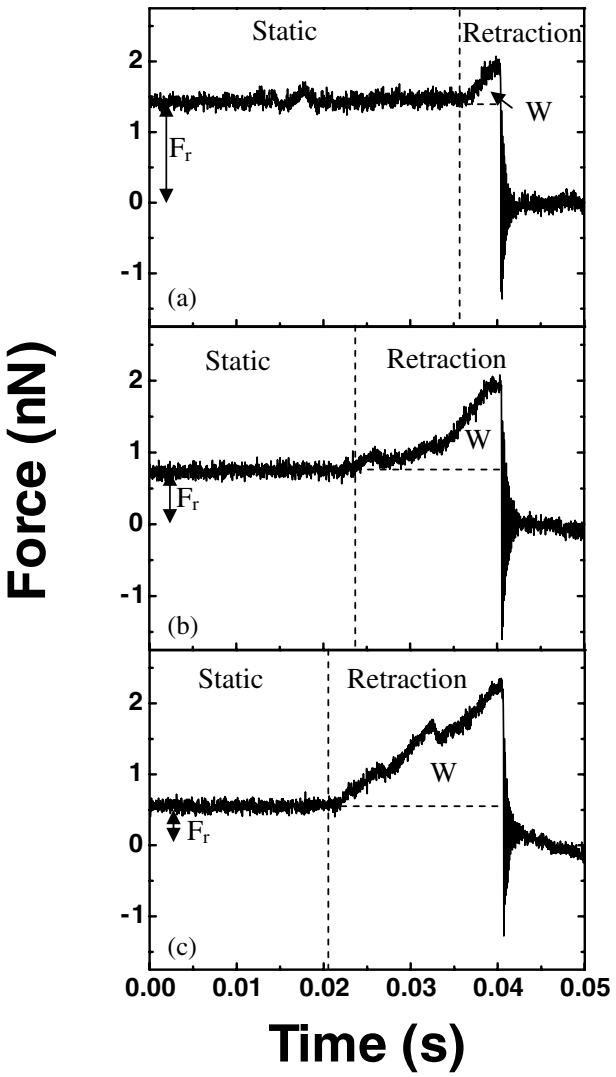

FIG. 2. Force profile for immersed single MWCNTs subsequently retracted, with rising positive force representing greater attraction, from (a) polyethylene glycol, (b) glycerol, and (c) water. The small bumps seen at 16, 26, 33 ms, respectively, can be related to environmental noise, and are not reproducible.

liquid, as follows:

$$\frac{\gamma_\ell(1+\cos\theta)}{2\sqrt{\gamma_\ell^d}} = \sqrt{\gamma_s^p}\left(\frac{\sqrt{\gamma_\ell^p}}{\sqrt{\gamma_\ell^d}}\right) + \sqrt{\gamma_s^d}, \qquad (2)$$

where γ_s is the surface tension of the solid, and superscripts d and p refer to the dispersive and polar contributions (γ_ℓ is the sum of the polar and dispersive components). A plot of Eq. (2), using the contact angles measured in this work and the literature values of the liquid surface tension components reported in Table I, is shown in Fig. 3. The excellent linearity of the plot supports the validity of the Owens-Wendt model here, and allows accurate determination of the nanotube dispersive and polar components: $\gamma_s^d = 17.6\ \mathrm{mJ\,m^{-2}}$ and $\gamma_s^p = 10.2\ \mathrm{mJ\,m^{-2}}$. The total surface tension $\gamma_s^d + \gamma_s^p$ ($=27.8\ \mathrm{mJ\,m^{-2}}$) of the nanotube is similar to that of an untreated graphite fiber ($=31.5\ \mathrm{mJ\,m^{-2}}$) [13](the curvature of which is essentially zero). The fact that single-walled nanotubes with diameters under 2.5 nm have been estimated [6] to have critical surface tension γ_c of 40–80 $\mathrm{mJ\,m^{-2}}$ is compatible with these results, considering the predicted effects of curvature [4]. The polar energy component ($10.2\ \mathrm{mJ\,m^{-2}}$) of the nanotube, however, is twice the $4.8\ \mathrm{mJ\,m^{-2}}$ measured for planar or fibrous graphite. Such increased polar interactions could explain why nanotubes are better wetted by water than graphite [14].

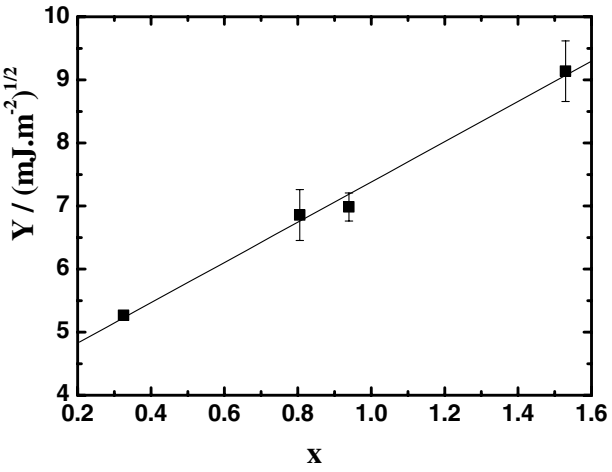

FIG. 3. Owens and Wendt plot for single MWCNTs. The y axis value Y represents $[\gamma_\ell(1+\cos\theta)]/2\sqrt{\gamma_\ell^d}$, and the x axis value X is $(\sqrt{\gamma_\ell^p}/\sqrt{\gamma_\ell^d})$. Each point is an average of at least five measurements, the error bar being the σ of each set of points.

Finally, the increase in attractive force (Fig. 2) during removal of carbon nanotubes from the liquids can be used to evaluate the mechanical distortion of the liquid meniscus. Since the wetting force is dependent only on the circumference of the interface [Equation (1)], which is approximately constant until separation, the increase in force during retraction may be associated only with the work done in deforming the liquid. This work, W, can be calculated directly from the triangular area under this curve and is shown in Table I. In contrast to the static wetting force discussed above, this force is *dynamic,* and is expected to vary with the retraction speed, a parameter we are currently unable to control. Still, the measured work increases with increasing liquid polarity, whereas a 3 orders of magnitude increase in viscosity from water to glycerol does not seem to significantly affect the work done to deform the liquid meniscus. This indicates that the effect is due to variations in the liquid free energy, and not dependent on viscous drag.

In conclusion, we have developed a method to precisely monitor the forces acting on individual carbon nanotubes during their immersion into and retraction from liquids

in air. The force profiles have been used to evaluate the equilibrium liquid contact angle using a Wilhelmy balance method. Contact angle data from this method reveals that the highly curved carbon structure modifies the wetting characteristics of the nanotube. Owens and Wendt plots reveal a significant increase in the polarity of the highly curved nanotube surface relative to planar graphite. The technique developed here also allows investigation of the liquid dynamics surrounding the pull-out event.

This project was supported by the (CNT) Thematic European network on "Carbon Nanotubes for Future Industrial Composites" (EU), the Minerva Foundation, the G. M. J. Schmidt Minerva Centre of Supramolecular Architectures, and the Israeli Academy of Science. We are grateful to S. Safran, P. Pincus, and M. Levy for their stimulating discussions, to J. E. Sader for providing software for cantilever calibration, and to R. Popovitz-Biro for the TEM picture.

[1] G. McHale, N. A. Kab, M. I. Newton, and S. M. Rowan, J. Colloid Interface Sci. **186**, 453 (1997).

[2] A. H. Barber, S. R. Cohen, and H. D. Wagner, Appl. Phys. Lett. **82**, 4140 (2003); P. M. Ajayan, L. S. Schadler, and P. V. Braun, *Nanocomposite Science and Technology* (Wiley-VCH, Weinheim, 2003), Chap. 2.

[3] Y. Gogotsi, J. A. Libera, A. Güvenç-Yazicioglu, and C. Megaridis, Appl. Phys. Lett. **79**, 1021 (2001).

[4] A. V. Neimark, J. Adhes. Sci. Technol. **13**, 1137 (1999).

[5] T. Werder *et al.*, Nano Lett. **1**, 697 (2002).

[6] E. Dujardin, T. W. Ebbesen, A. Krishnan, and M. M. J. Treacy, Adv. Mater. **10**, 1472 (1998).

[7] , in *Contact Angle, Wettability and Adhesion*, edited by K. L. Mittal (VSP, Utrecht, 1993), p. 235.

[8] J. Yamaki and Y. Katayama, J. Appl. Polym. Sci. **19**, 2897 (1975); B. J. Carroll, J. Colloid Interface Sci. **57**, 488 (1976); H. D. Wagner, J. Appl. Phys. **67**, 1352 (1990).

[9] F. Hoecker and J. Karger-Kocsis, J. Appl. Polym. Sci. **59**, 139 (1996); A. Ghenaim, A. Elachari, M. Louati, and C. Caze, J. Appl. Polym. Sci. **75**, 10 (2000).

[10] J. E. Sader, J. W. M. Chon, and P. Mulvaney, Rev. Sci. Instrum. **70**, 3967 (1999).

[11] H. Nishijima *et al.*, Appl. Phys. Lett. **74**, 4061 (1999).

[12] D. K. Owens and R. C. Wendt, J. Appl. Polym. Sci. **13**, 1741 (1969).

[13] G. M. Wu, J. M. Schultz, D. J. Hodge, and F. N. Cogswell, Polym. Compos. **16**, 284 (1995).

[14] A. W. Adamson, *Physical Chemistry of Surfaces* (Wiley, New York, 1990), 5th ed., p. 397.